Title

Myofibroblast proliferation and heterogeneity are supported by macrophages during skin repair.

Journal

Science, 362(6417)

Authors

Shook, Brett
Wasko, Renee
Rivera-Gonzalez, Guillermo
et al.

Publication Date

2018-11-23

DOI

10.1126/science.aar2971

Peer reviewed

HHS Public Access

Author manuscript

Science. Author manuscript; available in PMC 2019 August 06.

Published in final edited form as:

Science. 2018 November 23; 362(6417): . doi:10.1126/science.aar2971.

Myofibroblast proliferation and heterogeneity is supported by macrophages during skin repair

Brett A. Shook[1,*], **Renee R. Wasko**[1], **Guillermo C. Rivera Gonzalez**[1], **Emilio Salazar-Gatzimas**[2], **Francesc López-Giráldez**[3], **Biraja C. Dash**[4], **Andrés R. Muñoz-Rojas**[5], **Krystal D. Aultman**[1], **Rachel K. Zwick**[1], **Vivian Lei**[1], **Jack L. Arbiser**[6], **Kathryn Miller-Jensen**[1,5], **Damon A. Clark**[2], **Henry C. Hsia**[4], **Valerie Horsley**[1,7,*]

[1]Molecular, Cellular and Developmental Biology, Yale University, New Haven, CT 06511, USA

[2]Interdepartmental Neuroscience Program, Yale University, New Haven, CT 06511, USA

[3]Yale Center for Genome Analysis, Yale School of Medicine, New Haven, CT 06510, USA

[4]Department of Surgery (Plastic), Yale School of Medicine, New Haven, CT 06510, USA

[5]Department of Biomedical Engineering, Yale University, New Haven, CT 06511, USA

[6]Department of Dermatology, Atlanta Veterans Administration Health Center, Emory University, Atlanta, GA 30322, USA

[7]Department of Dermatology, Yale University, New Haven, CT 06511, USA

Abstract

During tissue repair, myofibroblasts produce extracellular matrix (ECM) molecules for tissue resilience and strength. Altered ECM deposition can lead to tissue dysfunction and disease. Identification of distinct myofibroblast subsets is necessary to develop treatments for these disorders. Here, using extensive analysis of pro-fibrotic cells during mouse skin wound healing, fibrosis and aging; we identify distinct subpopulations of myofibroblasts, including cells identified as adipocyte precursors (APs). Multiple mouse models and transplantation assays demonstrate that AP proliferation, and not other myofibroblasts, is activated by CD301b-expressing macrophages through IGF1 and PDGFC. With age, wound bed APs and differential gene expression between myofibroblast subsets are reduced. Our findings identify multiple fibrotic cell populations and suggest the environment dictates functional myofibroblast heterogeneity, which is driven by fibroblast-immune interactions after wounding.

One Sentence Summary:

During skin repair, macrophages activate proliferation of a myofibroblast subset with the capacity for adipocyte lineage and dermal repair.

Tissues sustain resilience and strength through maintenance of extracellular matrix (ECM) molecules by mesenchymal cells. Under disease states, pro-fibrotic conditions lead to

[*]Corresponding Author. brett.shook@yale.edu (B.A.S.); valerie.horsley@yale.edu (V.H.).

The authors have no competing interests.

excessive and disordered ECM deposition that impairs tissue function (1, 2). Additionally, dysregulated ECM is associated with aged skin and age-related defective wound healing (3–8). Variability in rates of wound healing, scarring, and fibrosis could result from functionally distinct mesenchymal cells (9, 10). Thus, identifying unique mesenchymal cell populations that contribute to fibrosis and the mechanisms that drive cellular diversity has significant implications for disease treatment (2, 11–13).

Prior experiments in mice have demonstrated that embryonic mesenchymal precursors expressing *Engrailed (En1)* or *Delta-like homolog 1* (*Dlk1/Pref1*) generate skin fibroblast and adipocyte lineages (14–16). During skin repair following injury, myofibroblasts expressing alpha smooth muscle actin (SMA), *Pdgfra, Sca1, Itga8, CD34* and *Dpp4* (CD26) migrate, proliferate, and deposit ECM (17–19). Myofibroblasts do not form lipid-filled adipocytes within regenerated tissue following standard small skin injury (14, 15, 20, 21), but can form adipocytes in large wounds that regenerate hair follicles (20). How environmental conditions alter functional cellular diversity and the contribution of mesenchymal subsets to tissue fibrosis are not well understood.

Here, we uncover unappreciated heterogeneity within wound bed myofibroblasts that is dependent on the tissue environment. In particular, we show the predominant population of myofibroblasts are adipocyte precursor cells (APs) derived from *En1*-lineage traced fibroblasts (14, 15, 21, 22) that contribute to tissue repair and ECM production/modulation. We show that, in wound beds of aged mice, APs are markedly reduced and wound bed myofibroblast subpopulations become more homogeneous in their gene expression profiles and localization. Our data indicate that CD301b$^+$ monocyte/macrophage-derived PDGFC and IGF signaling contributes to myofibroblast heterogeneity by selectively promoting the proliferation of wound bed APs and not other myofibroblast subsets. These findings define major subsets of wound bed myofibroblasts and identify immune and molecular interactions that promote functional cellular heterogeneity under distinct fibrotic conditions.

Mesenchymal cell heterogeneity under fibrotic conditions

Myofibroblasts within wound beds express PDGFRα, CD34 and Sca1, and derive from embryonic precursors that express *En1* or *Dlk1/Pref-1* (14–16) (14, 15, 23, 24) (Fig. 1A). Since PDGFRα, CD34 and Scal define APs (Sca1$^+$;CD34$^+$;CD29$^+$) (25, 26), we sought to determine if APs were derived from *En1*- and *Dlk1*-expressing precursors. We confirmed that *En1*Cre;*Rosa*26-LSL-tdTomato- and *Dlk1*CreER;mT/mG-traced cells expressed CD26 and Seal (14, 15) (Fig. 1B). Interestingly, 96% of tdTomato$^+$;Sca1$^+$;CD26$^+$ cells in *En*1Cre;tdTomato, and 97% of GFP$^+$;Sca1$^+$;CD26$^+$ cells in *Dlk*CreER;mTmG non-wounded skin express AP markers CD29 and CD34 (Fig. 1B and fig. S1).

Flow cytometry analysis of immune and endothelial lineage negative cells (Lin$^-$) isolated from uninjured dermis and 5-day wound beds revealed four populations of cells: CD29$^+$;CD34$^+$, CD34$^+$, CD29^{High} and CD29^{Low} cells (Fig. 1C). We define CD29$^+$;CD34$^+$ cells as APs since 90% retain Sca1$^+$ expression after injury and have adipogenic potential *in vitro* and *in vivo* (26–28) (fig. S2A). While AP and CD29^{Low} cells were the most abundant

populations in non-wounded skin, wound beds contained increased proportions of $CD29^{High}$ cells (Fig. 1C).

To determine which populations were myofibroblasts, we analyzed the expression of SMA and Collagen 1. Within wound beds, each cell population upregulated SMA and Collagen I mRNA expression compared to cell populations from uninjured skin (Fig. 1, D and E); however, flow cytometry revealed that only APs and $CD29^{High}$ cells were enriched for SMA, Col I and the fibroblast marker CD90 in wound beds (Fig. 1F).

To further analyze the fibrotic nature of these cell populations, we examined the expression of pro-fibrotic proteins Sca1, CD9, CD26 and PDGFRa (14–16, 22, 29) (fig. S1B and fig. S2, A to D). Interestingly, a greater percentage of APs, $CD29^{High}$, and $CD29^{Low}$ cells were $CD9^{+}$ after injury (fig. S2D), and $CD9^{+}$ APs have decreased *in vitro* adipogenic potential compared to $CD9^{-}$ APs (fig. S2, E and F). These data suggest that fibrotic cells are heterogeneous and distinct between uninjured and injured skin. Further, at least two major populations of fibrotic mesenchymal cells exist in skin wounds: APs and $CD29^{High}$ cells.

We next examined CD29 and CD34 populations in bleomycin-induced fibrosis. In contrast to wound healing, $CD29^{High}$ cells increased more robustly and fewer APs were observed after bleomycin treatment (fig. S2, G and H). Interestingly, colocalization with other pro-fibrotic markers was not dramatically changed (fig. S2, B to D). Thus, pro-fibrotic cellular composition in bleomycin-treated skin is distinct from wound healing, suggesting that unique strategies are required to treat tissue fibrosis under different pathological conditions.

Since SMA and CD9 expression increased in multiple populations of mesenchymal cells within skin wounds, we sought to design a comprehensive hierarchical marker panel to delineate mesenchymal heterogeneity in skin wounds using 6 fibrotic markers (Fig. 2, A and B and fig. S1). Immune and endothelial lineage negative cells (Lin^{-}) were subdivided based on PDGFRα and Scal (14, 15). While PDGF signaling is central to fibrosis (2, 21, 30–32), we included $PDGFR\alpha^{-}$ cells in our analysis since $PDGFR\alpha^{-}$ pro-fibrotic cells might also contribute to repair (14, 33). We further subdivided populations based on CD29 and CD34 expression and then by the presence of CD26 (High or Low) and CD9 (+/−). This analysis revealed that 54% of Lin^{-} cells in non-wounded skin contained surface markers that prospectively identify APs: $PDGFR\alpha^{+};Sca1^{+};CD29^{+};CD34^{+}$ (Fig. 2A, fig. S2A and fig. S3A). Within the AP pool, 66% were $CD26^{High};CD9^{-}$ (Fig. 2, A to C and fig. S4, A and B). The only other non-immune or non-vascular populations that contribute to greater than 3% of total cells in non-wounded skin were $PDGFR\alpha^{-};Sca1^{-};CD29^{High}$ ($CD29^{High}$) cells (~7 %) and $PDGFR\alpha^{-}$; $Sca1^{-};CD29^{Low}$ ($CD29^{Low}$) cells (~15%) (Fig. 2, A to C, fig. S2A and fig. S3A).

In 5-day wound beds, the relative abundance of APs decreased as $PDGFR\alpha^{+};CD29^{High}$ cells and $PDGFR\alpha^{-};Sca1^{-};CD29^{Low}$ cells became more abundant (Fig. 2, A to C, fig. S3 and fig. S4, A and B). Since $CD34^{+}$ cells were mostly SMA^{-} (Fig. 1F) and not abundant during repair, we excluded them from further analysis. $CD29^{High}$ and $CD29^{Low}$ cells remained predominantly $CD26^{Low};CD9^{+}$ and $CD26^{Low};CD9^{-}$, respectively (Fig. 2, A to C and fig. S4, A and B). Interestingly, 46% of APs were $CD26^{High};CD9^{+}$ in 5-day wound beds compared

to 24% in non-wounded skin (Fig. 2, A to C and fig. S4, A and B). The shift from $CD9^{-}$ to $CD9^{+}$ APs persisted 14 days after injury (fig. S3E). Immunofluorescent staining of FACS-isolated cells and wound beds showed greater intensity of CD26 staining in APs relative to other cells, confirming our flow cytometry results (fig. S4, C and D). SMA and Collagen 1 were expressed by APs and $CD29^{High}$ cells in wound beds regardless of their CD26 or CD9 expression; however, few $CD29^{Low}$ cells expressed SMA, Collagen 1, CD90 or ER-TR7 (Fig. 1, D to F, Fig. 2, D and E, and fig. S4, C to H).

To explore the spatial organization of myofibroblast subsets, we regionally dissected wound beds for flow cytometry and examined the signal intensity of CD26 and CD29 in non-immune ($CD45^{-}$) cells in tissue sections. While APs are found throughout the wound bed, $CD29^{High}$ cells were biased towards the most superficial region of the outer wound bed edge (Fig. 2F and fig. S5). Interestingly, $CD29^{High}$ cells were more abundant in the upper dermis of non-wounded skin, which contributes to the superficial regenerating dermis (15). Compared to mouse skin, human skin has a similar composition of mesenchymal cells. Yet surprisingly, a greater percentage of these populations were $CD26^{High}$ and $CD9^{+}$ (fig. S6), indicating that human skin may be more biased toward fibrotic responses.

To determine whether repair-related myofibroblast heterogeneity arises from conversion between cellular subsets, we performed genetic lineage tracing using inducible Cre-lox mouse lines that label pro-fibrotic cells: *Dlk1*CreER;mT/mG (postnatal labeling) and *Pdgfra*CreER;mT/mG (adult labeling) (fig. S7A) (15). In uninjured skin, several mesenchymal populations were labeled in *Dlk1*CreER mice, whereas *Pdgfra*CreER mice predominantly labeled APs (~94%) (fig. S7, B and C). *Pdgfra*CreER-lineage traced cells in 5-day wound beds contributed to APs, $Sca1^{-}$;$CD29^{Low}$ cells, and a rare population of $Sca1^{+}$;$CD29^{High}$ cells (fig. S7, C to F). $Sca1^{+}$;$CD29^{High}$ cells are $CD9^{+}$ during repair and similar in size to APs (fig. S7, E and F), suggesting they are pro-fibrotic. Two weeks after injury, *Pdgfra*CreER-lineage traced cells comprised ~80% APs, ~10% $Sca1^{+}$;$CD29^{High}$ cells, and 7% $Sca1^{-}$;$CD29^{Low}$ cells (fig. S7D). These data suggest that APs could contribute to multiple myofibroblast subpopulations; however, they do not contribute to the expansion of $Sca1^{-}$;$CD29^{High}$ cells. Yet, because non-AP, $CD29^{+}$ cells are labeled in *Pdgfra*CreER mice, we cannot rule out the possibility that proliferation of $CD29^{+}$ cells (fig. S12) also contributes to myofibroblast heterogeneity after injury.

Myofibroblast subsets have unique gene expression profiles

Comparison of transcriptional profiles of $CD29^{Low}$, $CD29^{High}$ cells and APs that were either CD9 positive or negative (AP – $CD9^{+}$ and AP – $CD9^{-}$) by RNA-sequencing (RNA-seq) (n=2 for each population, GSE105790) confirmed significant diversity among wound bed myofibroblasts (Fig. 3, A and B). While transcriptomic analysis revealed $CD9^{+}$ and $CD9^{-}$ APs were similar, each mesenchymal subset expressed unique mRNAs (fig. S8, fig. S9, and table S1). For instance, $CD29^{High}$ cells expressed elevated *Pdgfrβ, CD146, NG2* and other perivascular cell/pericyte markers (34) compared to APs and $CD29^{Low}$ cells and had elevated *Acta2* expression in non-wounded skin (Fig. 1D).

Although transcriptomes were distinct between cellular subsets, Ingenuity Pathway Analysis (IPA) predicted common active biofunctions and similar upstream activators of gene expression profiles (fig. S10, fig. S11, and table S2), suggesting some functional redundancy among myofibroblasts. However, many differentially expressed genes between APs and $CD29^{High}$ cells have been implicated in wound healing (Fig. 3C, fig. S8 and fig. S9). Additionally, each myofibroblast population was enriched for different ECM components and modifiers (Fig. 3C, fig. S8 and fig. S9). Interestingly, both $CD9^{+}$ and $CD9^{-}$ APs were enriched for many cytokines *(Ccl2, Cxcl1, Cxcl10* and *Cxcl12)* and ECM components *(Col5a2, Fbln1, Fbn1, Has1* and *Loxl1)* that promote rapid ECM deposition (35–37). Enrichment of genes involved in repair and fibrosis changed among myofibroblast populations between day 5 and day 14 of repair (fig. S8B), indicating that myofibroblast subsets can uniquely influence both the proliferative and maturation phases of tissue repair.

To determine whether myofibroblast subpopulations were functionally distinct, we examined collagen production, collagen crosslinking, and migration of APs and $CD29^{High}$ cells. We did not observe differences in collagen production or cellular migration; however, we detected an increased ability of APs to crosslink collagen compared to $CD29^{High}$ cells, consistent with elevated *Lox* expression in APs (Fig 3, C to F and fig. S8A).

Since myofibroblast numbers increase after injury (Fig. 1C and fig. S3), we examined *in vivo* proliferation within the different mesenchymal subsets (APs, $CD29^{High}$, and $CD29^{Low}$) during tissue repair. Proliferation increased in APs, $CD29^{High}$, and $CD29^{Low}$ cells after injury, and interestingly $CD26^{Low}$ cells were more proliferative than $CD26^{High}$ cells within each cellular subset (fig. S12, A to D). Taken together, these data demonstrate that the dermis contains tremendous heterogeneity within pro-fibrotic cells with distinct functions during tissue repair.

Myofibroblast composition and gene expression are altered during aging

Age-related defects in repair are associated with reduced myofibroblasts and dysfunctional ECM deposition (3–6) (fig. S13, A and B). To determine if mesenchymal populations were altered with age, we analyzed 5-day wound beds in young and aged mice. The relative abundance of APs decreased and $CD29^{High}$ cells increased in aged wound beds (Fig. 4, A to D), with reduced percentages of $CD9^{+}$ cells in all mesenchymal populations (Fig. 4C), suggesting that fibrotic cells are lost or not stimulated with age.

Analysis of transcriptional changes in myofibroblasts during aging by RNA-seq ($n = 2$, GSE105790) revealed fewer differentially expressed genes between myofibroblast subsets (fig. S14, A to C) due to an age-related down-regulation of many genes within individual populations (fig. S14D). Comparing the transcriptome of myofibroblast populations in young versus aged mice revealed age-related changes in gene expression of extracellular molecules (Fig. 4E) and increased expression of multiple metalloproteases in myofibroblasts, consistent with the ability of aged fibroblasts to break down ECM faster than young fibroblasts and impair healing (4, 6).

Adipocyte precursors become fibrotic after injury

To identify molecular mechanisms regulating AP myofibroblasts during repair, we isolated APs from uninjured skin and 5-day wound beds and performed RNA-seq ($n = 2$, GSE105788). Injury and repair upregulated *Acta2* (SMA) and several secreted factors implicated in tissue repair (fig. S15, A to C). Interestingly, several adipogenic genes and *in vitro* adipogenic potential were reduced in wound bed APs (fig. S15, D and E). Thus, APs displayed dramatic alterations within the wound environment that limit their adipogenic potential and promote myofibroblast gene expression, and could explain the myofibroblast origin of adipocytes in large wounds (20).

Macrophage signaling selectively activates proliferation of wound bed APs

Since delayed healing in aged mice is associated with decreased APs and APs rapidly increase from days 3 to 7 after injury when new dermal tissue is generated, we investigated potential signaling pathways that could impact AP numbers during repair. IPA predicted that injury-related changes in AP gene expression could result from monocyte/macrophage-derived ligands (fig. S15F). Macrophage ablation reduces wound bed myofibroblast numbers, impairs myofibroblast function and impairs wound healing (38–41); however, the underlying mechanisms are ill-defined. To examine the contribution of monocytes/macrophages to myofibroblast heterogeneity, we ablated macrophages using *LysM*Cre;iDTR mice (38, 41–43) (Fig. 5A). Surprisingly, ablating monocytes/macrophages reduced all AP subsets (fig. S16) and diminished AP proliferation in wounds without significantly changing $CD29^{High}$ or $CD29^{Low}$ populations (Fig. 5B and fig. S16A). Additionally, pharmacological reduction of macrophages decreased the percentage of dividing APs from 25% to 9% in controls (fig. S17), indicating that the myeloid lineage in 5-day wound beds selectively activates AP proliferation and not other myofibroblasts.

CD301b$^+$ macrophages activate AP proliferation during wound healing

During the mid-phase of wound healing (days 3–7), the myeloid lineage is predominantly comprised of monocyte and macrophage subsets (41, 44, 45) (fig. S18A). We have previously shown that wound bed macrophages expressing macrophage galactose-type C-type lectin 2 (*Mgl2*/CD301b) contributes to repair by promoting proliferation and fibroblast repopulation, and $CD301b^+$ macrophages are ablated in $Mgl2^{DTR}$ mice (41, 46, 47). While ablating all macrophages in *LysM*Cre;iDTR mice decreased proliferation of all subsets of APs, ablating CD301b-expressing macrophages reduced proliferation of $CD26^{Low}$ APs in 5-day wounds with no change in $CD29^{High}$ or $CD29^{Low}$ cell proliferation (Fig. 5C). This suggests that diversity in wound bed macrophages (48) allows proliferation of different AP subsets to be differentially regulated, thus promoting myofibroblast heterogeneity. Reduced AP proliferation in DT- treated $Mgl2^{DTR}$ mice resulted in a ~50% reduction in EdU^+ APs in 7-day wound beds that is only observed when newly generated $CD301b^+$ macrophages are ablated during the proliferative phase of repair (Fig. 5D). Consistent with this model, cell transplantation of $CD301b^+$ macrophages, and not other immune cells, increased AP proliferation (from 18% to 28%) while $CD29^{High}$ and $CD29^{Low}$ cells were unaltered (Fig. 5,

E and F). Further, cultured CD301b$^+$ macrophages doubled AP proliferation *in vitro* (Fig. 5G), demonstrating direct signaling between CD301b$^+$ macrophages and APs.

To identify signaling molecules that activate AP proliferation during repair, we compared the transcriptome of CD301b$^+$ macrophages to F4/80$^-$ immune cells isolated from day 5 wounds (Fig. 6A and fig. S18, B and C) (n = 2 per group, GSE105789). We identified ligands enriched in CD301b$^+$ macrophages that bind to receptors on APs (Fig. 6B and fig. S18D) and validated these results by quantifying protein secretion (fig. S18E). Cultured APs were treated with candidate molecules and only PDGFC and IGF1 induced proliferation (Fig. 6C). To determine if PDGFC and IGF1 signaling pathways contribute to AP proliferation *in vivo*, we administered ligand neutralizing antibodies or receptor antagonists after injury (Fig. 6D). Local injection of PDGFC or IGF1 neutralizing antibodies *in vivo* reduced AP proliferation; however, there was no detectable change in proliferation of other cells. Additionally, inhibition of PDGFRα and IGF1R or downstream PI3K signaling selectively reduced AP proliferation (Fig. 6D). Interestingly, we did not observe spatial biasing of CD301b$^+$ macrophages in wound beds (Fig. 6E) and gene expression of wound healing-associated genes changed minimally in myofibroblasts from 5-day wound beds of Mgl2^{DTR} mice relative to controls (fig. S19). These data suggests that the unique gene expression profile of each myofibroblast subset results from interactions with other tissue resident cells, such as keratinocytes (49). As a result, the delayed re-epithelialization and revascularization observed in Mgl2^{DTR} mice (41) could result from CD301b$^+$ macrophages interacting with keratinocytes and endothelial cells. IGF1 can stimulate repair, potentially through promoting migration and proliferation of keratinocytes and fibroblasts (35, 50–53), yet the contribution of PDGFC to healing has not previously been explored. To examine the contribution of PDGFC signaling to wound healing, we locally injected a PDGFC-neutralizing antibody at the periphery of wound beds and examined skin repair. We did not observe gross changes in re-revascularization and myofibroblast repopulation in 5-day wound beds compared to controls; however, we observed a slight decrease in re-epithelialization (fig. S20). These data demonstrate that multiple ligands produced by CD301b$^+$ macrophages activate proliferation of APs, and not other myofibroblast subsets, during wound healing.

Numbers of CD301b$^+$ macrophages increase in wounds as APs abundance increases (41). However, wound beds from aged mice contain fewer CD301b$^+$ cells compared to young controls and human keloid scars, which have been shown to contain many CD26$^+$ fibroblasts (54), and are enriched with CD301$^+$ cells (fig. S21). Thus, the interaction between CD301b$^+$ macrophages and mesenchymal cells may provide a therapeutic target for fibrosis-related diseases.

Discussion:

Dermal cells, including fibroblasts and adipocytes, support epidermal functions and integrity (11, 12). While a common embryonic precursor for SMA$^+$ wound bed myofibroblasts exists (14, 15, 20, 33, 55, 56), the diversity of mesenchymal cells during adult tissue repair is ill-defined. Here, we discovered that after injury, skin wound beds contain tremendous mesenchymal heterogeneity, similar to what is observed during lung fibrosis (57). We

identify two major classes of SMA^+ and Collagen I^+ myofibroblasts that arise from different cellular origins: cells with a cell surface marker profile of APs, and $CD29^{High}$ cells. Surprisingly, during tissue repair, a greater percentage of APs express pro-fibrotic cell surface proteins $CD26^{High}$ and $CD9^+$, with reduced adipogenic potential. Spatially, these two myofibroblast populations are distinct, with APs evenly distributed within wounds and $CD29^{High}$ cells biased towards superficial, outer regions of wound beds. RNA-sequencing and functional analysis of these myofibroblast subsets revealed that each subset has unique transcriptomes with some functional overlap.

With age, the abundance of APs decreases and $CD29^{High}$ cells are more prevalent, as differential gene expression is reduced between myofibroblast subsets. While myofibroblasts are dynamic after injury in mouse skin, human dermal fibroblasts express pro-fibrotic cell surface proteins in uninjured skin, possibly resulting in stronger fibrotic biasing humans. These studies illuminate unique functional subsets of fibrotic cells, providing a stepping-stone to develop therapeutic strategies that promote efficient wound healing and treat fibrosis.

Regulation of functional myofibroblast diversity

Here, we show that $CD26^{High}$ myofibroblasts are largely $CD34^+$;$CD29^+$ APs that function as myofibroblasts in regenerating mouse skin. While previous reports did not observe the same degree of $CD34^+$ and $CD29^+$ colocalization on myofibroblasts (14, 16), these differences likely result from changes in fibroblast surface marker expression associated with different ages and hair follicle stage (29). Our data reveal that biased proliferation and plasticity of fibroblast subsets promotes myofibroblast heterogeneity in skin wounds. Our lineage tracing data suggest a combination of proliferation and plasticity support fibroblast heterogeneity within regenerating skin.

While multiple signals likely influence myofibroblast heterogeneity, our study highlights the importance of myofibroblast-macrophage interactions, and particularly PDGFC and IGF1 in promoting myofibroblast heterogeneity and repair. These data resonate with the function of macrophages in tissue fibrosis (1, 58), the ability of exogenous PDGFC to rescue delayed skin wound healing in diabetic mice (59), and the promotion of fibroblast proliferation and repair by Igf1 (35, 50–53). In various tissues, macrophages express *Pdgfc* and *Igf1* following injury or under pathological conditions (60–64). Interestingly, Pdgf and Igf signaling cooperate synergistically to promote fibroblast proliferation and enhance wound healing without increasing scarring (65–67). Treatments aimed at fine-tuning the number of $CD301b^+$ macrophages could be of tremendous clinical value since reduction in $CD301b^+$ macrophages and CD26- expressing fibroblasts are associated with aging and defective wound, and keloid scars contain excessive ECM, CD26-expressing fibroblasts, and $CD301^+$ cells. Further understanding of how myofibroblast subsets function and are influenced by the microenvironment during fibrosis and pathologies with irregular ECM homeostasis will allow optimization of treatments for these encumbering diseases.

Supplementary Material

Refer to Web version on PubMed Central for supplementary material.

Acknowledgments:

This work was supported in part by NIH grants to V.H. from NIAMS (AR060295 & AR069550) and NIA through the pilot project grants from the Claude D. Pepper Older Americans Independence Center at Yale (NIA P30AG21342) awarded to V.H. B.A.S. is a New York Stem Cell Foundation - Druckenmiller Fellow. This research was supported by the New York Stem Cell Foundation. RNA sequencing data are available at the Gene Expression Omnibus (GEO) at www.ncbi.nlm.nih.gov/geo, under accession numbers GSE105788, GSE105789, GSE105790. We thank members of the Horsley lab, Dr. R. Atit and Dr. A. MacLeod for critical reading of the manuscript. We thank Dr. B. Hogan and Dr. C. Barkauskas for sharing *PdgfraCreER* mice and Dr. C. Wolfrum for sharing *Dlk1CreER* mice prior to the initial mouse line publications and Dr. R. Atit for *En1*Cre*Rosa26*-LSL-tomato mice.

References and Notes:

1. Wynn TA, Vannella KM, Macrophages in Tissue Repair, Regeneration, and Fibrosis. Immunity.44 450–462 (2016). [PubMed: 26982353]
2. Ebmeier S, Horsley V, Origin of fibrosing cells in systemic sclerosis. Current Opinion in Rheumatology. 27, 555–562 (2015). [PubMed: 26352735]
3. Gosain A, DiPietro LA, Aging and wound healing. World J Surg. 28, 321–326 (2004). [PubMed: 14961191]
4. Ballas CB, Davidson JM, Delayed wound healing in aged rats is associated with increased collagen gel remodeling and contraction by skin fibroblasts, not with differences in apoptotic or myofibroblast cell populations. Wound Repair Regen. 9, 223–237 (2001). [PubMed: 11472619]
5. Fujiwara T et al., Age-Associated Intracellular Superoxide Dismutase Deficiency Potentiates Dermal Fibroblast Dysfunction During Wound Healing. Exp. Dermatol. (2017), doi:10.1111/exd. 13404.
6. Vedrenne N, Coulomb B, Danigo A, Bonté F, Desmoulière A, The complex dialogue between (myo)fibroblasts and the extracellular matrix during skin repair processes and ageing. Pathologie Biologie. 60, 20–27 (2012). [PubMed: 22099331]
7. Naylor EC, Watson REB, Sherratt MJ, Molecular aspects of skin ageing. Maturitas. 69, 249–256 (2011). [PubMed: 21612880]
8. Kohl E, Steinbauer J, Landthaler M, Szeimies RM, Skin ageing. Journal of the European Academy of Dermatology and Venereology. 25, 873–884 (2011). [PubMed: 21261751]
9. Tabib T, Morse C, Wang T, Chen W, Lafyatis R, SFRP2/DPP4 and FMO1/LSP1 Define Major Fibroblast Populations in Human Skin. Journal of Investigative Dermatology. 138, 802–810 (2018). [PubMed: 29080679]
10. Philippeos C et al., Spatial and Single-Cell Transcriptional Profiling Identifies Functionally Distinct Human Dermal Fibroblast Subpopulations. Journal of Investigative Dermatology. 138, 811–825 (2018). [PubMed: 29391249]
11. Driskell RR, Watt FM, Understanding fibroblast heterogeneity in the skin. Trends in Cell Biology. 25, 92–99 (2015). [PubMed: 25455110]
12. Sorrell JM, Fibroblast heterogeneity: more than skin deep. Journal of Cell Biology. 117, 667–675 (2004).
13. Marangoni RG et al., Myofibroblasts in murine cutaneous fibrosis originate from adiponectin-positive intradermal progenitors. Arthritis Rheumatol. 67, 1062–1073 (2015). [PubMed: 25504959]
14. Rinkevich Y et al., Identification and isolation of a dermal lineage with intrinsic fibrogenic potential. Science. 348, aaa2151–aaa2151 (2015).
15. Driskell RR et al., Distinct fibroblast lineages determine dermal architecture in skin development and repair. Nature. 504, 277–281 (2013). [PubMed: 24336287]
16. Jiang D et al., Two succeeding fibroblastic lineages drive dermal development and the transition from regeneration to scarring. Nat Cell Biol, 1–19 (2018). [PubMed: 29269947]
17. Darby IA, Laverdet B, Bonté F, Desmoulière A, Fibroblasts and myofibroblasts in wound healing. CCID, 301 (2014).
18. Hinz B et al., Recent Developments in Myofibroblast Biology. AJPA. 180, 1340–1355 (2012).

19. Wynn TA, Ramalingam TR, Mechanisms of fibrosis: therapeutic translation for fibrotic disease. Nat Med. 18, 1028–1040 (2012). [PubMed: 22772564]
20. Plikus MV et al., Regeneration of fat cells from myofibroblasts during wound healing. Science, aai8792 (2017)
21. Iwayama T et al., PDGFRα signaling drives adipose tissue fibrosis by targeting progenitor cell plasticity. Genes Dev. 29, 1106–1119 (2015). [PubMed: 26019175]
22. Marcelin G et al., A PDGFRα-Mediated Switch toward CD9(high) Adipocyte Progenitors Controls Obesity-Induced Adipose Tissue Fibrosis. Cell Metabolism. 25, 673–685 (2017). [PubMed: 28215843]
23. Higashiyama R et al., Differential Contribution of Dermal Resident and Bone Marrow-Derived Cells to Collagen Production during Wound Healing and Fibrogenesis in Mice. J. Invest. Dermatol. 131, 529–536 (2011). [PubMed: 20962852]
24. Kanisicak O et al., Genetic lineage tracing defines myofibroblast origin and function in the injured heart. Nature Communications. 7, 1–14 (2016).
25. Berry R, Rodeheffer MS, Characterization of the adipocyte cellular lineage in vivo. Nat Cell Biol. 15, 302–308 (2013). [PubMed: 23434825]
26. Rivera-Gonzalez GC et al., Skin Adipocyte Stem Cell Self-Renewal Is Regulated by a PDGFA/AKT-Signaling Axis. Stem Cell. 19, 1–25 (2016).
27. Church CD, Berry R, Rodeheffer MS, Isolation and study of adipocyte precursors. Meth. Enzymol. 537, 31–46 (2014). [PubMed: 24480340]
28. Rodeheffer MS, Birsoy K, Friedman JM, Identification of white adipocyte progenitor cells in vivo. Cell. 135, 240–249 (2008). [PubMed: 18835024]
29. Lichtenberger BM, Mastrogiannaki M, Watt FM, -catenin activation remodels the dermis via paracrine signalling to distinct fibroblast lineages. Nature Communications. 7, 1–13 (2016).
30. Ostendorf T, Eitner F, Floege J, The PDGF family in renal fibrosis. Pediatr. Nephrol. 27, 1041–1050 (2011). [PubMed: 21597969]
31. Reigstad LJ, Varhaug JE, Lillehaug JR, Structural and functional specificities of PDGF-C and PDGF-D, the novel members of the platelet-derived growth factors family. FEBS J. 272, 5723–5741 (2005). [PubMed: 16279938]
32. Bonner JC, Regulation of PDGF and its receptors in fibrotic diseases. Cytokine & Growth Factor Reviews. 15, 255–273 (2004). [PubMed: 15207816]
33. Dulauroy S, Di Carlo SE, Langa F, Eberl GER, Peduto L, Lineage tracing and genetic ablation of ADAM12+ perivascular cells identify a major source of profibrotic cells during acute tissue injury. Nat Med. 18, 1262–1270 (2012). [PubMed: 22842476]
34. Paquet-Fifield S et al., A role for pericytes as microenvironmental regulators of human skin tissue regeneration. Journal of Clinical Investigation, 1–12 (2009).
35. Werner S, Grose R, Regulation of wound healing by growth factors and cytokines. Physiol. Rev. 83, 835–870 (2003). [PubMed: 12843410]
36. Ding J, Tredget EE, The Role of Chemokines in Fibrotic Wound Healing. Advances in Wound Care. 4, 673–686 (2015). [PubMed: 26543681]
37. Xue M, Jackson CJ, Extracellular Matrix Reorganization During Wound Healing and Its Impact on Abnormal Scarring. Advances in Wound Care. 4, 119–136 (2015). [PubMed: 25785236]
38. Goren I et al., A Transgenic Mouse Model of Inducible Macrophage Depletion. AJPA. 175, 132–147 (2010).
39. Lucas T et al., Differential Roles of Macrophages in Diverse Phases of Skin Repair. Journal of Immunology (Baltimore, Md. : 1950). 184, 3964–3977 (2010).
40. Mirza R, DiPietro LA, Koh TJ, Selective and Specific Macrophage Ablation Is Detrimental to Wound Healing in Mice. AJPA. 175, 2454–2462 (2010).
41. Shook B, Xiao E, Kumamoto Y, Iwasaki A, Horsley V, CD301b+ Macrophages Are Essential for Effective Skin Wound Healing. J. Invest. Dermatol. 136, 1885–1891 (2016). [PubMed: 27287183]
42. Burkhardt CB,C, Reith W, Renkawitz R, Forster I, Conditional gene targeting in macrophages and granulocytes using LysMcre mice. Transgenic research. 8, 265–277 (1999). [PubMed: 10621974]

43. Buch T et al., A Cre-inducible diphtheria toxin receptor mediates cell lineage ablation after toxin administration. Nature Publishing Group 2, 419–426 (2005).
44. Daley JM, Brancato SK, Thomay AA, Reichner JS, Albina JE, The phenotype of murine wound macrophages. Journal of Leukocyte Biology. 87, 59–67 (2010). [PubMed: 20052800]
45. Mirza R, Koh TJ, Dysregulation of monocyte/macrophage phenotype in wounds of diabetic mice. Cytokine. 56, 256–264 (2011). [PubMed: 21803601]
46. Kumamoto Y et al., CD301b+ Dermal Dendritic Cells Drive T Helper 2 Cell-Mediated Immunity. Immunity. 39, 1–11 (2013). [PubMed: 23890059]
47. Yang Bin et al., IL-27 Facilitates Skin Wound Healing through Induction of Epidermal Proliferation and Host Defense. J. Invest. Dermatol. 137, 1166–1175 (2017). [PubMed: 28132857]
48. Hu MS et al., Delivery of monocyte lineage cells in a biomimetic scaffold enhances tissue repair. JCI Insight. 2 (2017), doi:10.1172/jci.insight.96260.
49. Werner S, Krieg T, Smola H, Keratinocyte-fibroblast interactions in wound healing. Journal of Investigative Dermatology. 127, 998–1008 (2007). [PubMed: 17435785]
50. Ando Y, Jensen PJ, Epidermal Growth Factor and Insulin-Like Growth Factor I Enhance Keratinocyte Migration. J. Invest. Dermatol. 100, 633–639 (1993). [PubMed: 8491986]
51. Haase I, Evans R, Pofahl R, Watt FM, Regulation of keratinocyte shape, migration and wound epithelialization by IGF-1- and EGF-dependent signalling pathways. Journal of Cell Biology. 116, 3227–3238 (2003).
52. Simmons JG, Pucilowska JB, Keku TO, Lund PK, IGF-I and TGF-beta1 have distinct effects on phenotype and proliferation of intestinal fibroblasts. Am J Physiol Gastrointest Liver Physiol. 283, G809–18 (2002). [PubMed: 12181198]
53. Rudman SM, Philpott MP, Thomas GA, Kealey T, The Role of IGF-I in Human Skin and its Appendages: Morphogen as Well as Mitogen? J. Invest. Dermatol. 109, 770–777 (1997). [PubMed: 9406819]
54. Xin Y et al., Expansion of CD26 positive fibroblast population promotes keloid progression. Exp. Cell Res. 356, 104–113 (2017). [PubMed: 28454879]
55. Suga H et al., Tracking the Elusive Fibrocyte: Identification and Characterization of Collagen-Producing Hematopoietic Lineage Cells During Murine Wound Healing. STEM CELLS. 32, 1347–1360(2014) [PubMed: 24446236]
56. Hinz B, Formation and Function of the Myofibroblast during Tissue Repair. Journal of Investigative Dermatology. 127, 526–537 (2007). [PubMed: 17299435]
57. Rock JR et al., Multiple stromal populations contribute to pulmonary fibrosis without evidence for epithelial to mesenchymal transition. Proc Natl Acad Sci USA. 108, E1475–83 (2011). [PubMed: 22123957]
58. Vannella KM, Wynn TA, Mechanisms of Organ Injury and Repair by Macrophages. Annu. Rev. Physiol. 79, annurev-physiol-022516–034356 (2016).
59. Gilbertson DG et al., Platelet-derived Growth Factor C (PDGF-C), a Novel Growth Factor That Binds to PDGF a and p Receptor. J Biol Chem. 276, 27406–27414 (2001). [PubMed: 11297552]
60. Triantafyllopoulou A et al., Proliferative lesions and metalloproteinase activity in murine lupus nephritis mediated by type I interferons and macrophages. Proc Natl Acad Sci USA. 107, 3012–3017 (2010). [PubMed: 20133703]
61. Chang HR, Kim HJ, Xu X, Ferrante AW Jr., Macrophage and adipocyte IGF1 maintain adipose tissue homeostasis during metabolic stresses. Obesity. 24, 172–183 (2015). [PubMed: 26663512]
62. Ramachandran P et al., Differential Ly-6C expression identifies the recruited macrophage phenotype, which orchestrates the regression of murine liver fibrosis. Proc Natl Acad Sci USA. 109, E3186–95 (2012). [PubMed: 23100531]
63. Tonkin J et al., MonocytelMacrophage-derived IGF-1 Orchestrates Murine Skeletal Muscle Regeneration and Modulates Autocrine Polarization. Mol Ther. 23, 1189–1200 (2015). [PubMed: 25896247]
64. Pohlers D, Huber R, Ukena B, Kinne RW, Expression of platelet-derived growth factors C and D in the synovial membrane of patients with rheumatoid arthritis and osteoarthritis. Arthritis & Rheumatism. 54, 788–794 (2006). [PubMed: 16508943]

65. Lynch SE, Nixon JC, Colvin RB, Antoniades HN, Role of platelet-derived growth factor in wound healing: synergistic effects with other growth factors. Proc Natl Acad Sci USA. 84, 7696–7700 (1987). [PubMed: 3499612]

66. Lynch SE, Colvin RB, Antoniades HN, Growth factors in wound healing. Single and synergistic effects on partial thickness porcine skin wounds. Journal of Clinical Investigation. 84, 640–646 (1989). [PubMed: 2788174]

67. Lynch SE et al., The effects of short-term application of a combination of platelet-derived and insulin-like growth factors on periodontal wound healing. J. Periodontol. 62, 458–467 (1991). [PubMed: 1920013]

68. Chung M-I, Bujnis M, Barkauskas CE, Kobayashi Y, Hogan BLM, Niche-mediated BMP/SMAD signaling regulates lung alveolar stem cell proliferation and differentiation. Development. 145, dev163014–22 (2018).

69. Schwalie PC et al., A stromal cell population that inhibits adipogenesis in mammalian fat depots. Nature, 1–28 (2018).

70. Conway J et al., Inhibition of colony-stimulating-factor-1 signalingin vivo with the orally bioavailable cFMS kinaseinhibitor GW2580, 1–10 (2005).

71. Priceman SJ et al., Targeting distinct tumor-infiltrating myeloid cells by inhibiting CSF-1 receptor: combating tumor evasion of antiangiogenic therapy. Blood. 115, 1461–1471 (2010). [PubMed: 20008303]

72. Festa E et al., Adipocyte Lineage Cells Contribute to the Skin Stem Cell Niche to Drive Hair Cycling. Cell. 146, 761–771 (2011). [PubMed: 21884937]

73. Schmidt BA, Horsley V, Intradermal adipocytes mediate fibroblast recruitment during skin wound healing. Development. 140, 1517–1527 (2013). [PubMed: 23482487]

74. Tadeu AMB et al., Transcriptional Profiling of Ectoderm Specification to Keratinocyte Fate in Human Embryonic Stem Cells. PLoS ONE. 10, e0122493 (2015).

75. Trapnell C et al., Differential gene and transcript expression analysis of RNA-seq experiments with TopHat and Cufflinks. Nat Protoc. 7, 562–578 (2012). [PubMed: 22383036]

76. Wynn TA et al., Quantitative assessment of macrophage functions in repair and fibrosis. Curr Protoc Immunol. Chapter 14, Unit14.22 (2011).

77. Mirza RE, Fang MM, Ennis WJ, Koh TJ, Blocking interleukin-1 p induces a healing-associated wound macrophage phenotype and improves healing in type 2 diabetes. Diabetes. 62, 2579–2587 (2013). [PubMed: 23493576]

78. McGee HM et al., IL-22 Promotes Fibroblast-Mediated Wound Repair in the Skin. Journal of Investigative Dermatology. 133, 1321–1329 (2012). [PubMed: 23223145]

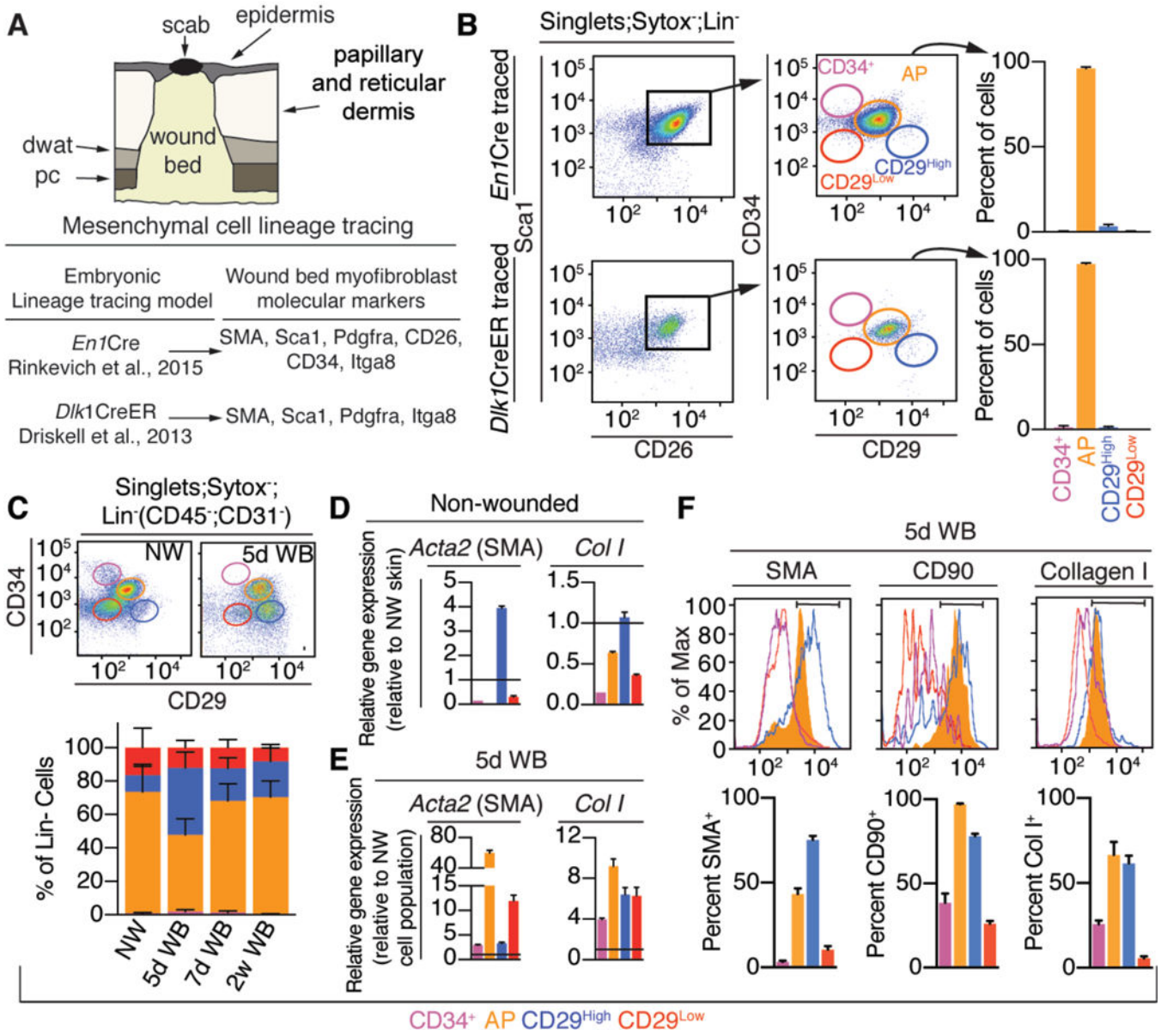

Fig. 1. Dermal mesenchymal cell heterogeneity changes after injury.

(A) Identified molecular markers of wound bed myofibroblasts using genetic lineage tracing. **(B)** FACS analysis and quantification of CD34 and CD29 subsets of Sca1^{+};CD26^{High} lineage traced cells in non-wounded skin ($n = 4$). **(C)** FACS plots and quantification of cellular subsets in non-wounded ($n = 8$), 5-day ($n = 19$), 7-day ($n = 4$) and 14-day wound beds ($n = 7$). (**D** and **E**) Real-time qPCR analysis of SMA (*Acta2*) and Collagen I (*Col I*) in mesenchymal subsets isolated from non-wounded skin **(D)** or 5-day wound beds **(E)**. **(F)** Representative flow cytometry histograms and quantification of SMA, CD90 and Collagen I in mesenchymal subsets ($n = 3$). Error bars indicate mean ± SEM. *$p < 0.05$, **$p < 0.01$, ***$p < 0.001$, ****$p < 0.0001$. NW, non-wounded; WB, wound bed; pc, panniculus carnosus; dwat, dermal white adipose tissue.

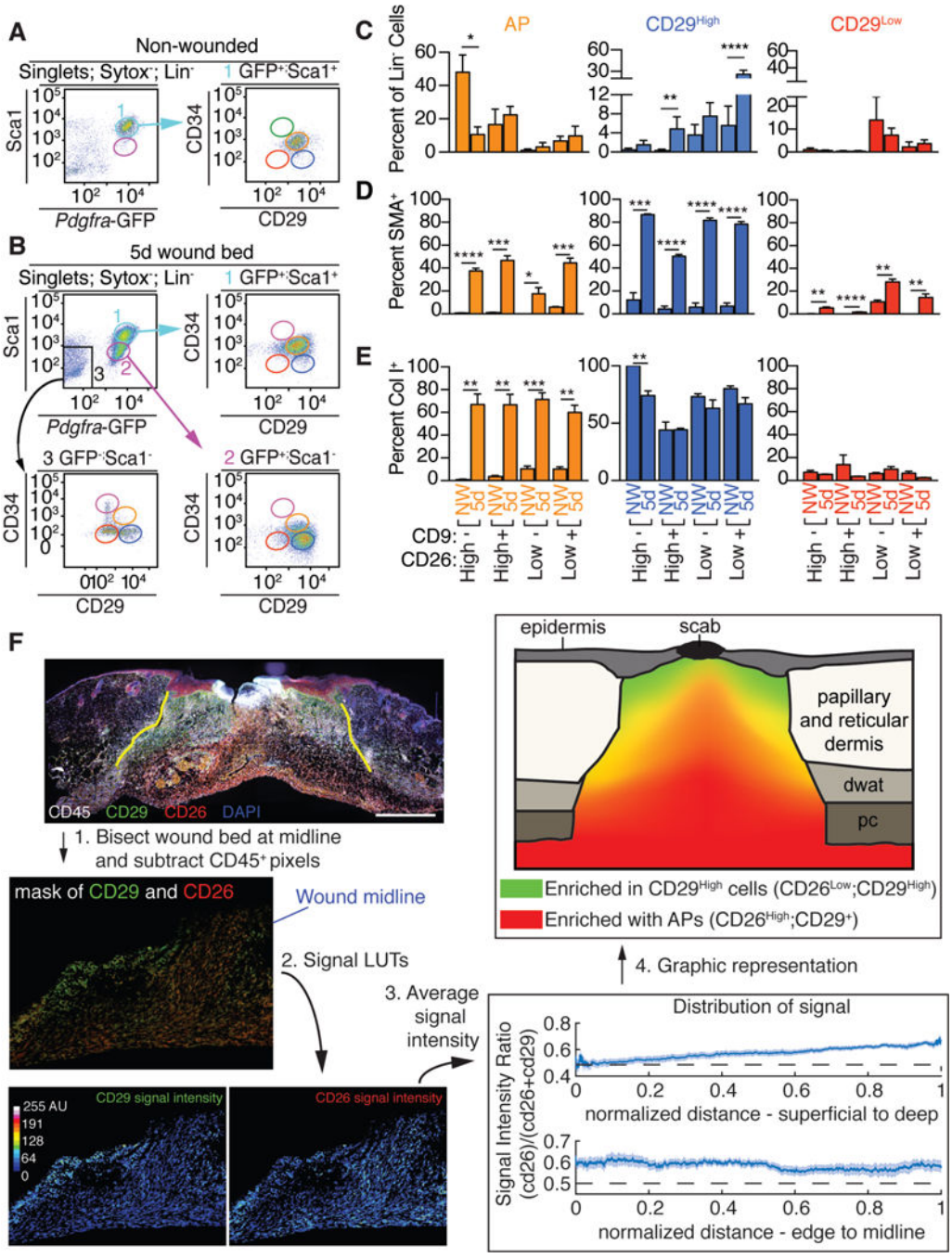

Fig. 2. Skin wounds contain multiple myofibroblast subsets.

(A and **B)** FACS plots detailing the gating strategy to define mesenchymal subpopulations. **(C** to **E)** Quantification of the relative abundance of prevalent pro-fibrotic subsets ($n = 6$) **(C)** and colocalization with SMA **(D)** and Collagen I **(E)** in non-wounded and 5-day wound bed mesenchymal subsets ($n = 3$). **(F)** Pipeline for processing immunostained tissue sections to infer the location of APs ($CD29^{+}$;$CD26^{High}$) and $CD29^{High}$ cells in day 5 wound beds. Yellow lines delineate wound edges. Scale bar, 250μm. Error bars indicate mean ± SEM. *$p < 0.05$, **$p < 0.01$, ***$p < 0.001$, ****$p < 0.0001$. NW, non-wounded; WB, wound bed; pc,

panniculus carnosus; dwat, dermal white adipose tissue; AU, arbitrary units; LUT, look up table.

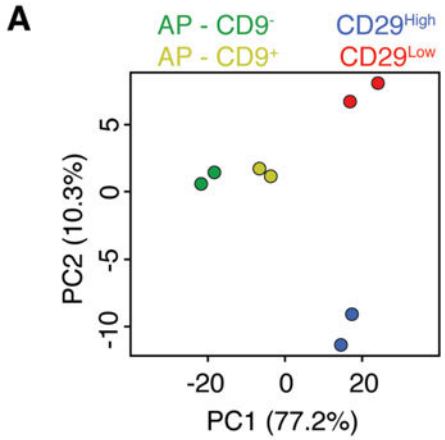

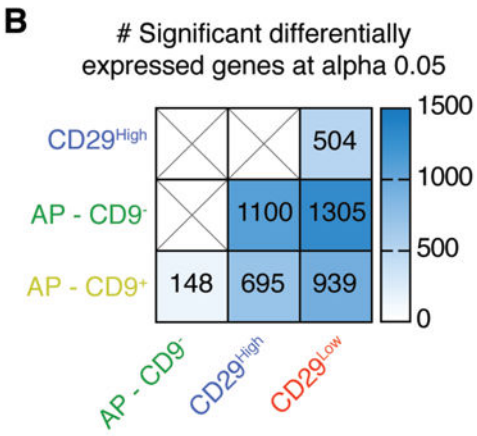

C

	Enriched in APs vs CD29^{High}	Enriched in CD29^{High} vs APs
Extracellular molecules	*Ccl2, Ccl7, Ccl11, Csf1, Cxcl1, Cxcl2, Cxcl10, Cxcl12, Cxcl13, Cxcl14, Figf, Gas6, Il6, Il33, Nov, Ogn, Sfrp4, Timp1, Vasn, Wisp2, Wnt2*	*Ccl3l3, Ccl6, Gdf15, Hbegf, Inhba, Il1A, Il1B, Il1rn, Pdgfa, Pf4 (Cxcl4), Spp1 (Opn), Tgfb2, Tnf, Vegfc, Wnt5A*
Receptors	*Adora2b, Cxcr7*, Dpp4 (Cd26), Il6st*, Il11ra*, Il13ra1*, Lpar1*, Osmr1*, Pdgfra*, Sfrp2, Sfrp4, Tgfbr2, Tgfbr3*	*Ccr2, Endra, Endrb, Fgfr4*, Il2rg, Il10ra, Itgam, Itgb2*, Pdgfrb*
ECM components/ regulators	*Adamts1, Adamts2, Adamts4, Adamts5, Col5a2, Col14a1, Fbln1, Fbn1, Has1, Loxl1, Mmp2, Mmp3, Mmp23, Mmp27, Plod2, Podn, Timp3*	*Adamtsl2, Col6a3, Col7a1, Col12a1, Mmp13, Tnc*

* Predicted upstream activators of unique gene expression profiles

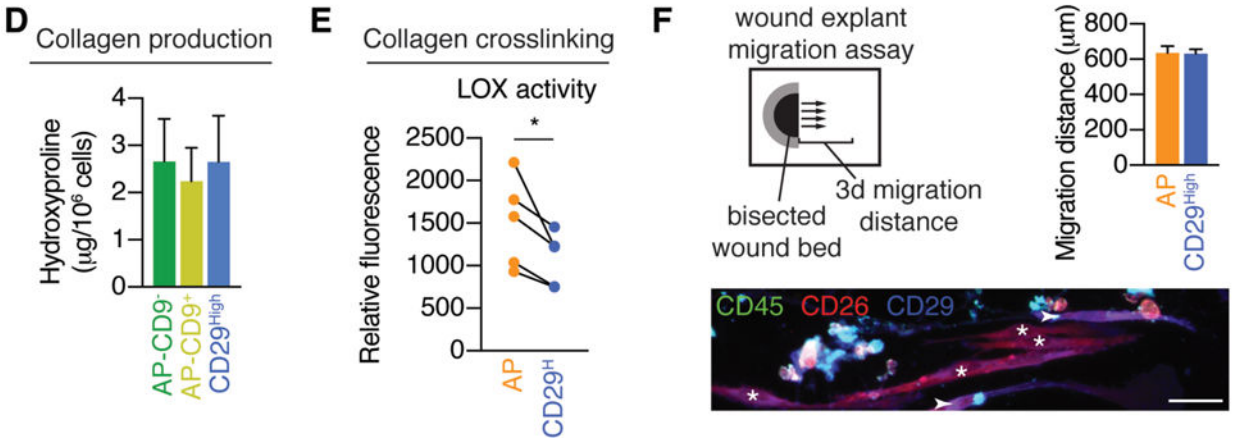

Fig. 3. Myofibroblast subsets can distinctively regulate repair.

(A) Transcriptomic PCA of myofibroblast subsets. **(B)** Table of statistically significant, differentially expressed genes between cellular subsets. **(C)** Wound healing-related genes enriched in APs (CD9^{-} and CD9^{+} AP populations) or CD29^{High} cells. **(D** and **E)** Quantification of hydroxyproline content ($n = 7$) **(D)** and lysyl oxidase (LOX) activity in cells from day 5 wounds ($n = 4$; $p = 0.0416$) **(E)**. **(F)** Migration distance of APs (CD26^{High}) (asterisks) and CD29^{High} cells (arrow heads) from cultured wound beds ($n \geq 250$ cells from 3 wound beds). Scale bar, 10µm. Error bars indicate mean ± SEM.

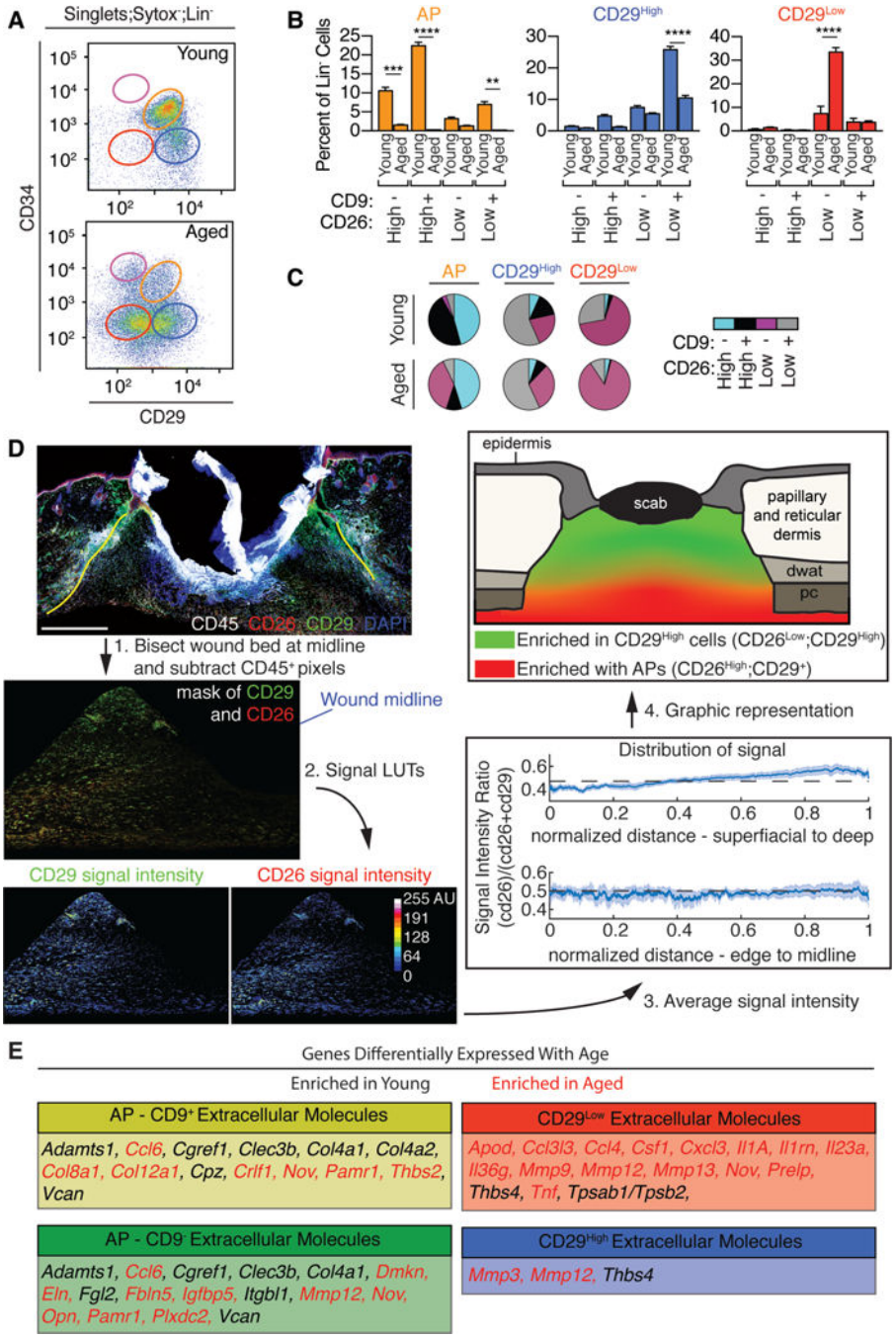

Fig. 4. Myofibroblast composition and gene expression is altered during aging.

(A) FACS plots from 5-day wounds from young and aged mice. **(B)** Quantification of the relative abundance of prevalent pro-fibrotic subsets in 5-day wounds ($n = 4$). **(C)** Pie charts depicting CD9 and CD26 colocalization. **(D)** Pipeline for processing immunostained wound bed sections to infer APs and CD29^{High} cell location in day 5 wound beds from aged mice. Yellow lines delineate wound edges. Scale bar, 250μm. **(E)** Genes with altered differential expression with age. Black and red text indicates enrichment in young and aged mice, respectively. Error bars indicate mean ± SEM. pc, panniculus carnosus; dwat, dermal white

adipose tissue; AU, arbitrary units; LUT, look up table. $^{**}p < 0.01$, $^{***}p < 0.001$, $^{****}p < 0.0001$.

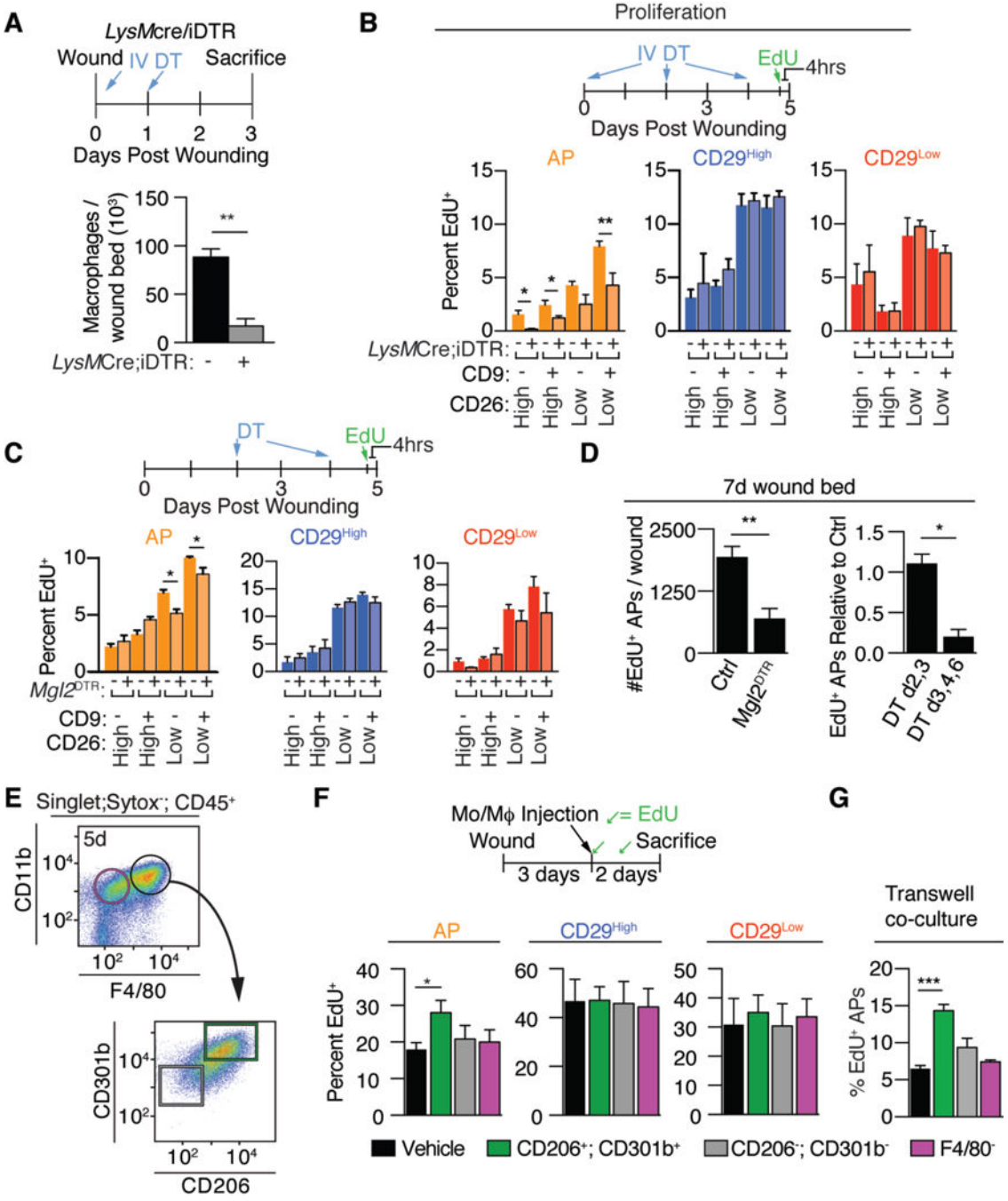

Fig. 5. CD301b^{+} macrophages selectively stimulate AP proliferation during wound healing.

(**A**) Quantification of wound bed macrophages depletion ($n \geq 3$; $p = 0.004$). **(B)** Quantification of myofibroblast proliferation in wound beds ($n = 4$). **(C)** Quantification of cell proliferation in wound beds of CD301b^{+} macrophage-depleted mice (*Mgl2*^{DTR}) ($n = 3$). **(D)** Quantification of EdU-incorporating APs in mice receiving DT on day 2, 4 and after injury (left) ($n = 3$, $p = 0.0469$) and DT 2 and 3 or 3, 4 and 6 days after injury (right) (n = 3, $p = 0.0116$). Mice were given 2 injections of EdU per day from day 3 thru 7 after injury. **(E)** FACS plots of immune cell populations isolated for transplants. **(F** and **G)** Quantification of

EdU-incorporating cells after injection of select immune cell subsets *in vivo* ($n = 5$, $p = 0.0146$) **(F)** or Transwell co-culture **(G)** (n = 6, $p = 0.001$). Error bars indicate mean ± SEM. *$p < 0.05$, **$p < 0.01$.

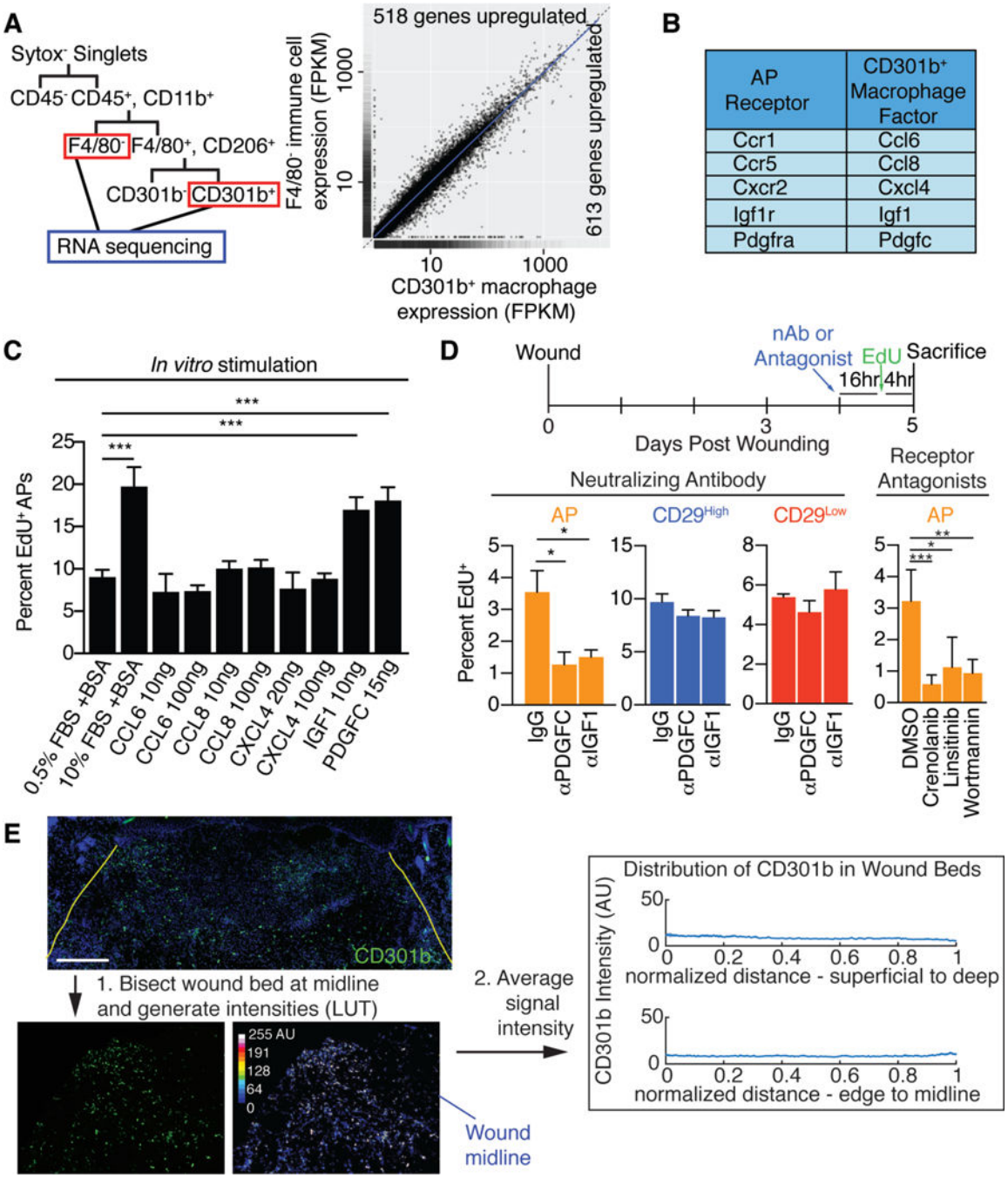

Fig. 6. CD301b$^+$ macrophage-derived ligands activate AP proliferation.

(A) Cell populations isolated from 5-day wound beds for RNA-sequencing (left) and FPKM scatterplot (right). **(B)** Table of ligands enriched in CD301b$^+$ macrophages that bind to receptors on APs. **(C)** Quantification of AP proliferation following administration of ligands. 10% FBS is a positive control ($n = 5$, ***$p < 0.001$). **(D)** Quantification of *in vivo* cellular proliferation after administration of PDGFC ($n = 6$, $p = 0.0337$) and IGF1 ($n = 6$, $p = 0.0436$) neutralizing antibodies or antagonists against PDGFRα (Crenolanib) ($n = 6$, p=0.0001), IGFR1 (Linsitinib) ($n = 4$, $p = 0.01017$) or PI3K (Wortmannin) ($n = 4$, $p =$

0.0028). **(E)** Pipeline for processing immunostained wound bed sections to infer the distribution of $CD301b^+$ macrophages in day 5 wounds ($n = 6$). Yellow lines delineate wound edges. Scale bar, 250μm. Error bars indicate mean ± SEM.